UV−Vis Absorption, Luminescence, and X-ray Photoelectron Spectroscopic Studies of Rhodamine Dyes Adsorbed onto Different Pore Size Silicas

L. F. Vieira Ferreira,* M. J. Lemos, M. J. Reis, and A. M. Botelho do Rego

Centro de Química-Física Molecular-Complexo Interdisciplinar, Instituto Superior Técnico, 1096 Lisboa Codex, Portugal

Received June 24, 1999. In Final Form: March 29, 2000

Sulforhodamine 101 and rhodamine 6G were adsorbed onto silicas with different pore sizes ranging from 22 to 150 Å. Ground-state diffuse reflectance absorption spectra revealed the formation of different forms of adsorbed sulforhodamine 101 depending on concentration and on the pore size of the silica. For low loadings (0.001 to about 0.025 μmol of dye/g of silica) the absorption spectra are broad, hypsochromically shifted in relation to the monomer spectra, and quite different from the ethanolic solution spectra. For high loadings (0.050 to about 0.20 μmol g^{-1}) they are similar to the solution spectra with a small shift of about 7 nm. For rhodamine 6G spectra are much more "solution type" in the entire range of concentrations under study (0.001 to about 0.20 μmol g^{-1}). The "weighed" fluorescence quantum yields ($\sum_i f_i \phi_{F_i}$) determined for sulforhodamine 101 were 0.10 ± 0.03, 0.35 ± 0.05, and 0.50 ± 0.10 for low loadings and for 25, 60, and 150 Å silicas, respectively. For high loadings $\sum_i f_i \phi_{F_i} = 0.70 \pm 0.10$. These values for $\sum_i f_i \phi_{F_i}$ can be compared with a value of about 0.70 obtained for rhodamine 6G in all silicas (low loadings) and a unitary ϕ_F for high loadings. X-ray photoelectron spectroscopic studies present clear evidence for multiple occupation of the pores for all silicas under study. Surface concentration is quite independent of dye loading, although it changes from silica to silica. These studies indicate that sulforhodamine 101 forms nonplanar conformers in small pore size silicas as compared to large pore silica samples where the amount of conformers being formed is reduced. Rhodamine 6G samples exhibit very little conformer formation, but their ϕ_F is still slightly dependent on pore size. Both rhodamines exhibit smaller fluorescence quantum yields when compared to the case of adsorption onto microcrystalline cellulose, this effect being more relevant in the sulforhodamine 101 case.

1. Introduction

In the past decade we have made some surface photochemical studies of several dyes, including rhodamines, adsorbed onto a scarcely used adsorbent: powdered cellulose. Room-temperature luminescence, triplet−triplet energy transfer, and electron and hydrogen transfer as well as the nature of the adsorption process were studied (see refs 1−3 and references quoted therein).

The effect of the pore size on the kinetics of an electron-transfer process on the silica surface was also studied.[2]

Rhodamines and related xanthene dyes have been extensively studied in solution.[4−8] Both molecular structure and solvent play very important roles in the nonradiative pathways of deactivation of the first excited state of these dyes.[4−8] The cationic forms of rhodamine B, rhodamine 6G, and rhodamine 101 in acidic ethanol present different fluorescent emission quantum yields. For rhodamine B $\phi_F = 0.49$ and this efficiency varies strongly with temperature, while for the latter compound ϕ_F is unitary and independent of temperature.[4,5] The amino groups in rhodamine B are fully ethylated while in rhodamine 101 the amino groups are rigidly attached to the xanthene ring by methylenic bridges. Rhodamine 6G dissolved in ethanol has a $\phi_F = 0.95$;[4] in this case the amino groups are only partially substituted by ethyl groups.

The precise interpretation of the mechanism of internal conversion appears not to be completely established. On the basis of rotation about the xanthene−amine bond, Drexhage proposed, in the 1970s,[4] an intramolecular rotation model, which was later disputed by other research groups. Rettig and co-workers proposed a twisted intramolecular charge-transfer mechanism (TICT; electron transfer from the amino group to the xanthene moiety, followed by rotation about the xanthene−amine bond) as the main mechanism for nonradiative deactivation.[6]

* To whom correspondence should be addressed. Tel.: 351-21 841 92 52. Fax: 351-21 846 44 55. E-mail: LFVieiraFerreira@ist.utl.pt.

(1) (a) Vieira Ferreira, L. F. *Quimica* **1999**, *72*, 28. (b) Vieira Ferreira, L. F.; Freixo, M. R.; Garcia, A. R.; Wilkinson, F. *J. Chem. Soc., Faraday Trans.* **1992**, *88*, 15. (c) Vieira Ferreira, L. F.; Garcia, A. R.; Freixo, M. R.; Costa, S. M. B. *J. Chem. Soc., Faraday Trans.* **1993**, *89*, 1937. (d) Vieira Ferreira, L. F.; Netto-Ferreira, J. C.; Khmelinskii, I. V.; Garcia, A. R.; Costa, S. M. B. *Langmuir* **1995**, *11*, 231.

(2) Levin, P. P.; Costa, S. M. B.; Vieira Ferreira, L. F. *J. Phys. Chem.* **1996**, *100*, 15171.

(3) (a) Vieira Ferreira, L. F.; Cabral, P. V.; Almeida, P.; Oliveira, A. S.; Reis, M. J.; Botelho do Rego, A. M. *Macromolecules* **1998**, *31*, 3936. (b) Botelho do Rego, A. M.; Penedo Pereira, L.; Reis, M. J.; Oliveira, A. S.; Vieira Ferreira, L. F. *Langmuir* **1997**, *13*, 6787.

(4) (a) Drexhage, K. H. In *Dye Lasers*; Schafer, F. P., Ed.; Springer: Berlin, 1973; Vol. 1, p 144. (b) Drexhage, K. H. *J. Res. Natl. Bur. Stand., Sect. A* **1976**, *80A*, 421. (c) Arden, J. A.; Deltau, G.; Huth, U.; Peros, D.; Drexhage, K. H. *J. Lumin.* **1991**, *48, 49*, 352.

(5) (a) Kartens, T.; Knobs, K. *J. Phys. Chem.* **1980**, *84*, 1871. (b) Ferguson, J.; Mau, A. W. H. *Aust. J. Chem.* **1973**, *24*, 1617. (c) Sadowski, P. J.; Fleming, G. R. *Chem. Phys. Lett.* **1978**, *57*, 526. (d) Arden, J.; Deltan, G.; Huth, V.; Kringed, U.; Peros, D.; Drexhage, K. H. *J. Lumin.* **1991**, *48, 49*, 352.

(6) (a) Vogel, M.; Retttig, W.; Sens, R.; Drexhage, K. H. *Chem. Phys. Lett.* **1988**, *147*, 461. (b) *Ibid.*, p 452.

(7) (a) López Arbeloa, T.; Estévez, M. J.; López Arbeloa, F.; Urretxa Aguirresacona, I.; López Arbeloa, I. *J. Lumin.* **1991**, *48, 49*, 400. (b) López Arbeloa, F.; López Arbeloa, T.; Tapia Estévez, M. J.; López Arbeloa, I. *J. Phys. Chem.* **1991**, *95*, 2203. (c) López Arbeloa, F.; Urretxa Aguirresacona, I.; López Arbeloa, I. *Chem. Phys.* **1989**, *130*, 371. (d) López Arbeloa, I.; Rohatgi-Mukherjee, K. K. *Chem. Phys. Lett.* **1986**, *129*, 607. (e) López Arbeloa, I.; Rohatgi-Mukherjee, K. K. *Chem. Phys. Lett.* **1986**, *128*, 474.

(8) (a) Casey, K. G.; Onganer, Y.; Quitevis, E. L. *J. Photochem. Photobiol. A: Chem.* **1992**, *64*, 307. (b) Casey, K. G.; Quitevis, K. E. *J. Phys. Chem.* **1988**, *92*, 6590.

10.1021/la9908182 CCC: $19.00
Published on Web 05/27/2000

Chart 1

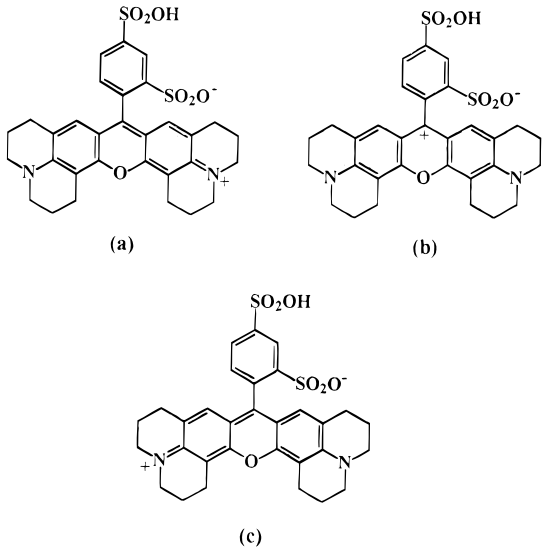

Chart 1 shows the most important resonance contributors of the acid form of sulforhodamine 101. López Arbeloa et al.[7] and others,[8] in an interesting series of papers on rhodamine dyes, claimed that internal conversion may be associated with a change from planar (and fluorescent) structure to a pyramidal and nonfluorescent one upon absorption of a photon. As a result of this umbrella-like motion (ULM) the positive charge moves from the amino group to the xanthene group and the double bond character of the xanthene amino group is lost. The electron system is interrupted, and the amino group may rotate after excitation.

The picture described so far for rigid and nonrigid rhodamines applies essentially to solution, either in high-viscosity or in low-viscosity solvents.

In the solid state the photophysics of rhodamines may be markedly different from solution.[9,10] As an example, rhodamine 101 shows a monoexponential decay in ethanol (τ_F in ethanol is 4.3 ± 0.1 ns).[9] Adsorption onto dry microcrystalline cellulose does not change the lifetime of the probe.[9] Adsorption on silica or glass with distorted adsorption sites markedly decreases the observed lifetime of rigid and nonrigid rhodamines.[10b]

As adsorbents, several types of porous silica were used in the present work. They are amorphous and granular forms of synthetic silica, consisting of a complex network of microscopic pores that attract and entrain water or organic compounds by means of physical adsorption.[11−13]

This work concerns electronically inert surfaces and not electronically active surfaces.[13b] So recent information on silica gel surface properties and rhodamine dyes on surfaces is included rather than a summary of recent literature data on other oxide gels.

Porous silica has a spongelike structure from which large surface areas result, which vary enormously with pore size (20−750 $m^2\ g^{-1}$). The surface area corresponds primarily to the area of the internal pore walls.[11,12] The average pore size of each silica is commonly obtained from surface area measurements. Since even the smallest pores are larger than most molecules but of the same order of magnitude, restrictions in what concerns molecular mobility are not unexpected. The surface of the porous silica consists of a network of silanol (Si−OH) and siloxane (Si−O−Si) groups with physically adsorbed water. This physically adsorbed water on silica can be removed by submitting it to moderate heating under vacuum, while the removal of chemiadsorbed water (reducing the number of SiOH groups in the surface) requires high temperatures.[11c,d]

Surface hydroxyl groups are extremely important in the process of surface adsorption, and it has been suggested that the smaller the pore of the silica, the larger the percentage of active silanols relative to the total number of silanols per unit of the surface area.[11b]

X-ray photoelectron spectroscopy (XPS) is a powerful tool for surface characterization. The technique is strongly surface sensitive due to the photoelectron escape depth: only the first 10−20 atomic surface layers can be analyzed.[14a] XPS is capable of providing information about elemental concentration profiles by angle-resolved analysis only for nearly ideal surfaces: flat, smooth, nonporous, homogeneous in the plane of the surface, nonvolatile, conductive, and stable with respect to ultrahigh vacuum. Silicas are far from fulfilling these criteria. However, despite these difficulties, a lot of interesting work with porous materials[3,15,16] has recently been reported. As an example, experimental evidence for hydrogen bond formation between a cyanine dye and cellulose was presented, involving the dye nitrogen atom.[3b]

Following previous studies of rhodamine dyes,[1b,c,3a] in this paper we report spectroscopic information regarding sulforhodamine 101 and rhodamine 6G when adsorbed onto silicas with different pore sizes. Samples will be compared from the point of view of UV−vis ground-state diffuse reflectance measurements as well as steady-state luminescence studies, providing a close insight into the nature of the interactions between the porous silica substrate and the probes.

With the use of the XPS technique and more specifically through the study of the nitrogen 1s photoelectron region, conclusions can be drawn regarding the existence of intermolecular interactions between the dye and the substrate and concerning the molecular conformations.

With these studies we hope to gain insight into the nature of the interactions of sulforhodamine 101 and rhodamine 6G with the substrate inside the pores. We aim to establish clear differences between the two physically adsorbed rhodamines in what concerns the possible

(9) (a) Vieira Ferreira, L. F.; Lemos, M. J. Unpublished results. (b) Lemos, M. J.; Vieira Ferreira, L. F. Photophysical Properties of Rhodamine Dyes Adsorbed onto Wet and Dry Microcrystalline Cellulose. In *Eurolights II-Light on Organized Molecular Systems*; Hengelhoef, Belgium, 1995; p 90.

(10) (a) Kemnitz, K.; Murao, T.; Yamazaki, I.; Nakashima, N.; Yoshihara, K. *Chem. Phys. Lett.* **1983**, *101*, 337. (b) Kemnitz, K.; Tamai, N.; Yamazaki, I.; Nakashima, N.; Yoshihara, K. *J. Phys. Chem.* **1987**, *91*, 1, 1423.

(11) (a) Turro, N. J. *Tetrahedron* **1987**, *43*, 1589. (b) Snyder, L. R.; Ward, J. W. *J. Phys. Chem.* **1966**, *70*, 3941. (c) De Mayo, P.; Natarajan, L. V.; Ware, W. R. in *Organic Phototransformations in Nonhomogeneous Media*; Fox, M. A., Ed.; American Chemical Society: Washington, DC, 1985; pp 1−19. (d) Nawrocki, J. *J. Chromatogr.* **1997**, *779*, 29.

(12) (a) Leigh, W. J.; Johnson, L. In *Handbook of Organic Photochemistry*; Scaiano, J. C., Ed.; CRC Press: Boca Raton, FL, 1989; Vol. 2, Chapter 22, p 401 and references therein. (b) Unger, K. K. *Porous Silica*; Elsevier: Amsterdam, 1979. (c) Iler, L. *The Chemistry of Silica*; Wiley: New York, 1979.

(13) (a) Aldrich Technical Information Bulletin, No. AL-144. (b) Kamat, P. *Chem. Rev.* **1993**, *93*, 267.

(14) (a) Briggs, D.; Seah, M. S. In *Practical Surface Analysis by Auger and X-ray Photoelectron Spectroscopy*; John Wiley & Sons Ltd.: Chichester, U.K., 1983. (b) Wagner, C. D. NIST X-ray Photoelectron Database, U.S. Department of Commerce, NIST, 1989.

(15) (a) Desaeger, M.; Reis, M. J.; Botelho do Rego, A. M.; Lopes da Silva, J. D.; Verpoest, I. *J. Mater. Sci.* **1996**, *31*, 6305. (b) Reis, M. J.; Botelho do Rego, A. M.; Lopes da Silva, J. D.; Soares, M. N. *J. Mater. Sci.* **1995**, *30*, 118.

(16) (a) Bradley, R. H.; Sutherland, I.; Sheng, E. *J. Colloid Interface Sci.* **1996**, *179*, 561. (b) Garbassi, F.; Balducci, L.; Chiurlo, P.; Deiana, L. *Appl. Surf. Sci.* **1995**, *84*, 145.

formation of new species, which may have a strong influence in the luminescence of the probes.

2. Experimental Section

2.1. Materials and Sample Preparation. Sulforhodamine 101 and rhodamine 6G (chloride) were purchased from Radiant Dyes Chemie, in the highest purity available. Ethanol was from Merck (gradient grade for liquid chromatography) and was dried with molecular sieves (Aldrich, 4 Å, 4−8 mesh). Rhodamines were laser dyes used without further purification after checking their purities by means of UV−vis absorption spectra (ϵ_{max} in the visible was compatible with literature data) and thin-layer chromatography (one spot on Kieselgel 60F254 from Merck). All the solvents were used as received, after checking their purities by UV and visible optical absorption spectrophotometry.

As adsorbents, different grades of Aldrich silicas were purchased: grade 12 for the 22 Å pore size silica; grades 923, 634, and 644 for the 25, 60, and 150 Å pore sizes, respectively. For 40 and 100 Å pore size, Merck silicas were used. Whenever possible the 100−200 mesh particle size (150−75 μm) was bought. In cases where this particle size was not commercially available (22, 40, and 100 Å silicas) we used sieves to separate that specific particle size range from the lot. Retsch sieves (stainless steel, with the appropriated wire gauze) were used. Silicas were dried at 110 °C under reduced pressure ($\sim 10^{-3}$ mbar) for 24 h prior to use for sample preparation (or kept in a desiccator under vacuum until they were used).

Samples were prepared as follows: Type I samples or *deposited samples* occur where the rhodamines were adsorbed from the ethanolic solution by very slow solvent evaporation (~48 h). In this case, samples were prepared as described in refs 1b−d except for the final solvent removal step which was performed in an acrylic chamber with two electrically heated shelves (Heto, models FD 1.0-110 and FC-2R/H) with temperature control (40 ± 1 °C) and reduced pressure (ca. 10^{-3} mbar, 12 h). The solvent used for sample preparation was ethanol. Type II samples or *equilibrium samples* occur where the solution of the dye in ethanol is allowed to stay in equilibrium with the dried silica powder for at least 24 h. After removal of the supernatant solution, its dye concentration was evaluated by absorption spectrometry, allowing us to calculate (by subtraction) the amount of dye that stayed adsorbed onto the silica surface.

For comparison purposes, other samples were also prepared, by repeatedly washing type I samples with ethanol until no significative amount of dye was found in the washing alcohol. The use of ground-state diffuse reflectance (GSDR) absorption spectrophotometry allowed us to evaluate the amount of dye that stayed adsorbed on the silica.

2.2. Ground-State Absorption Spectra in the UV−Vis Regions: Steady-State Emission Experiments. Ground-state absorption studies of the two rhodamines adsorbed on silica or microcrystalline cellulose were performed using a OLIS 14 UV−vis−NIR spectrophotometer with a diffuse reflectance attachment. The integrating sphere is 90 mm in diameter and internally coated with a standard white coating. The standard apparatus was modified to include the possibility of using short-wave-pass filters (Corion 600-S or 550-S) which excludes the two rhodamines luminescence from reaching the detector (Hamamatsu, model R955).

Further experimental details and a description of the system calibration used to obtain accurate reflectance measurements are given in refs 1b,c.

Solution absorption measurements were made using the same apparatus in the normal transmission mode.

Corrected steady-state fluorescence and phosphorescence emission spectra of the rhodamines under study, adsorbed on silica or microcrystalline cellulose, were obtained using a homemade fluorometer previously described.[17]

2.3. XPS Experiments. For X-ray photoelectron spectroscopy (XPS) studies, type I samples were mounted on the sample stub using a double-sided tape. Samples were analyzed by X-ray photoelectron spectroscopy (XPS) using a XSAM800 (Kratos) X-ray spectrometer operated in the fixed analyzer transmission (FAT) mode, with a pass energy of 20 eV, a power of 130 W, and the nonmonochromatized Mg Kα X-radiation ($h\nu = 1253.7$ eV). Typical base pressure in the ultrahigh vacuum (UHV) analysis chamber was in the range of 10^{-9} mbar. All sample transfers were made in air. Samples were analyzed at room temperature, at a takeoff angle of 0° relative to the normal of the surface. Spectra were collected and stored in 300 channels with a step of 0.1 eV using a Sun SPARC Station 4 and with Vision software (Kratos). The curve fitting for component peaks was carried out with a nonlinear least-squares algorithm using a mixture of Gaussian and Lorentzian peak shapes and Shirley background.

Charge shifts due to the insulating character of samples were corrected through the Si 2p silica component centered at 103.1 eV.[14b]

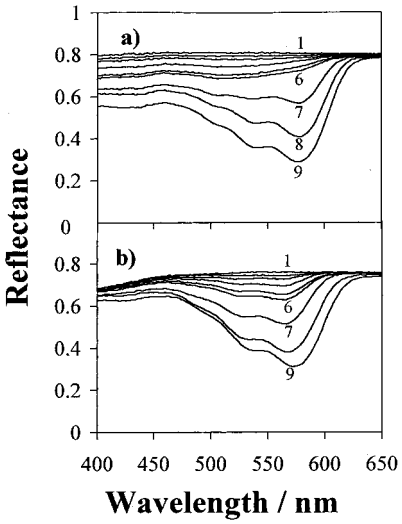

Figure 1. Reflectance spectra of sulforhodamine 101 adsorbed onto different pore size silicas. "Type I" samples are from ethanolic solutions. (a) Silica 22 Å: curve 1, the blank; curve 2, 0.001 μmol g^{-1}; curve 3, 0.002 μmol g^{-1}; curve 4, 0.005 μmol g^{-1}; curve 5, 0.0075 μmol g^{-1}; curve 6, 0.010 μmol g^{-1}; curve 7, 0.025 μmol g^{-1}; curve 8, 0.050 μmol g^{-1}; curve 9, 0.075 μmol g^{-1}. (b) Silica 150 Å: curve 1, the blank; curve 2, 0.001 μmol g^{-1}; curve 3, 0.002 μmol g^{-1}; curve 4, 0.004 μmol g^{-1}; curve 5, 0.0075 μmol g^{-1}; curve 6, 0.010 μmol g^{-1}; curve 7, 0.025 μmol g^{-1}; curve 8, 0.050 μmol g^{-1}; curve 9, 0.075 μmol g^{-1}.

3. Results and Discussion

3.1. Ground-State Absorption Spectra of Sulforhodamine 101 and Rhodamine 6G Adsorbed onto Powdered Silica. Figure 1a shows the spectral reflectance (R) versus wavelength for sulforhodamine 101 adsorbed onto 22 Å silica from ethanol (type I samples), while Figure 1b shows similar curves for the 150 Å silica. In all these cases, solutions of different concentrations were used for sample preparation, thus enabling us to compare different loadings of the dye on different silicas. The curves represent the reflectance as a function of wavelength in the range 400−650 nm. For shorter wavelengths (300 nm) the absorption of the dye is masked by the intrinsic absorption of silica. It is interesting to note that similar concentrations provide quite different reflectance spectra and that absorption of the adsorbed sulforhodamine seems to be more "solution type" for larger loadings of the dye.

There is a clear concentration dependence in what concerns the shape of the spectra: lower loadings seem to provide broader as well as hypsochromically shifted absorption bands for sulforhodamine 101, this effect being more important the smaller the silica pore. This behavior does not exist for rhodamine 6G as we will show later. For

(17) (a) Vieira Ferreira, L. F.; Costa, S. M. B.; Pereira, E. J. *J. Photochem. Photobiol., A: Chem.* **1991**, *55*, 361. (b) Vieira Ferreira, L. F.; Costa, S. M. B. *J. Lumin.* **1991**, *48, 49*, 395.

both dyes, the highest loadings (about 0.20 μmol/g) present some evidence for H dimer formation (sandwich dimers[1]).

Small pore silicas seem to evidence an increase in the absorption at shorter wavelengths. In the 22 Å silica the monomer maximum absorption (~575 nm) can be hardly seen in curves 1−6, while for 150 Å silica the monomer is quite evident. These reflectance spectra together with data for the remission function presented further in Figure 4 show that the 60 Å silica seems to be an intermediate situation.

The remission function $F(R)$ is obtained by calculating the Kubelka−Munk function for optically thick samples, i.e., those where any further increase in thickness does not affect the experimentally determined reflectance R.[18]

$$F(R) = \frac{(1 - R)^2}{2R} = \frac{K}{S} \qquad (1)$$

K and S are the absorption and scattering coefficients with dimensions (distance)$^{-1}$. For an ideal diffuser, where the radiation has the same intensity in all directions, $K = 2\epsilon C$ (ϵ is the Naperian absorption coefficient, C is the concentration).[18] Since the substrate usually absorbs at the excitation wavelength λ_e,

$$F(R)_{\text{probe}} = F(R)_{\text{total}} - F(R)_{\text{sil}} = \frac{2\sum_i \epsilon_i C_i}{S} \qquad (2)$$

where $F(R)_{\text{sil}}$ is the blank obtained with a cell containing only silica. This equation predicts a linear relation for the remission function of the probe versus concentration (for a constant scattering coefficient) whenever the probe is simply in the form of a monomer. In this case, however, S varies from silica to silica. We used the method reported by Oelkrug et al.[19] for the experimental determination of scattering coefficients, determining R as a function of the sample width. We obtained 22.0 ± 2.0, 15.0 ± 1.5, 12.5 ± 1.5, 11.0 ± 1.5, and 10.0 ± 1.5 cm^{-1} for the 25 (or 22), 40, 60, 100, and 150 Å silicas, respectively.

Initially we tried to correlate $F(R)$ with the concentration of dye in terms of moles per gram of silica for all the silicas under use; in this case we found linear correlations but with different slopes for each silica and for both dyes. However, by taking also into account the void space in each silica, this means by multiplying C (μmol g^{-1}) by the density in grams per cubic centimeter, we obtained a unique slope for all the silicas in the case of rhodamine 6G ($F(R)$ versus $C(d/S)$ in units of μmol cm^{-2}), as we show in Figure 2 (top).

The decadic extinction coefficient determined in this case (for rhodamine 6G at the wavelength used for fluorescence excitation, λ = 495 nm, by the use of eq 2) was $\epsilon = (5.8 \pm 0.4) \times 10^4$ mol^{-1} L cm^{-1} and is the same for all the silica substrates used here. In the case of rhodamine 6G entrapped within the polymer chains of microcrystalline cellulose, $\epsilon = (6.1 \pm 0.1) \times 10^4$ mol^{-1} L cm^{-1}. For an ethanolic solution of rhodamine 6G, $\epsilon = (3.0 \pm 0.3) \times 10^4$ mol^{-1} L cm^{-1} at 495 nm. Different hosts seem to provide similar extinction coefficients for the adsorbed rhodamine 6G.

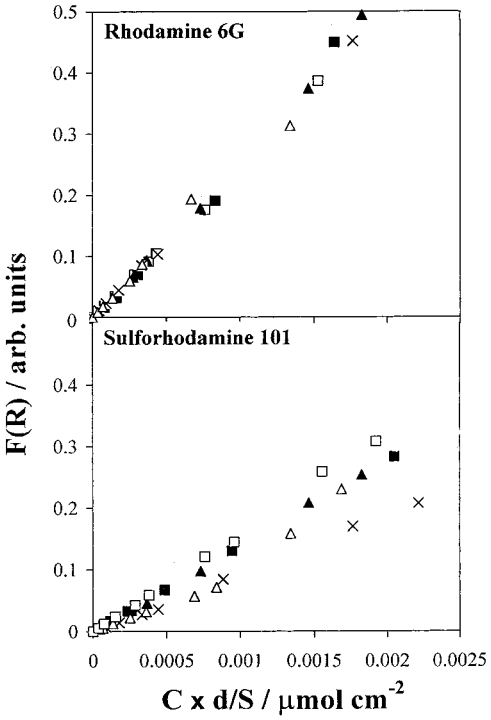

Figure 2. Remission function values, $F(R)$, as a function of $C(d/S)$ (see text) for rhodamine 6G and sulforhodamine 101 adsorbed onto silica with (□) 150 Å, (△) 100 Å, (■) 60 Å, (×) 40 Å, and (△) 25 Å pore diameters. $F(R)$ is measured at 495 nm for rhodamine 6G and at 540 nm for sulforhodamine 101.

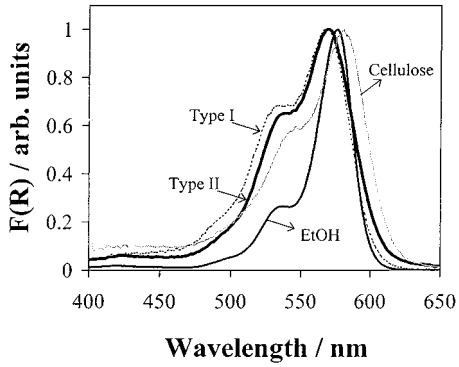

Figure 3. Remission function values for sulforhodamine 101 adsorbed, normalized to the maximum of the absorption of the dye: type I sample onto silica 150 Å with 0.051 μmol g^{-1}; type II sample onto silica 150 Å with 0.050 μmol g^{-1}; diluted ethanolic solution of the dye containing only monomers (~10^{-5} mol L^{-1}); dye adsorbed onto microcrystalline cellulose with 0.100 μmol g^{-1}.

Figure 2 (bottom) also shows that the same correlation (at λ = 540 nm in this case) could not be found for sulforhodamine 101. In this case each silica provides its slope ($F(R)$ versus $C(d/S)$). These data (ϵ varying with the silica pore size), as well as other data we will show later, indicate that we are no longer in the presence of a unique absorbing species.

Figure 3 shows the remission function of type I samples for sulforhodamine 101 onto 150 Å silica (0.05 mol of dye/g of the substrate) and type II samples for sulforhodamine 101 with the same concentration and on the same silica. A diluted solution of this dye in ethanol containing only monomers and a solid sample using microcrystalline cellulose (0.10 mol g^{-1}) as substrate are also presented.

(18) Wilkinson, F.; Kelly, G. P. In *Handbook of Organic Photochemistry*; Scaiano, J. C., Ed.; CRC Press: Boca Raton, FL, 1989; Vol. 1, p 293 and references therein.

(19) (a) Kortum, G.; Oelkrug, D. *Z. Naturforch.* **1964**, *19a*, 28. (b) Oelkrug, D.; Kortum, G. *Z. Phys. Chem. (Munich)* **1968**, *58*, 181. (c) Wendlandt, W.; Hecht, H. G. *Reflectance Spectroscopy*; Interscience Publishers: New York, 1966; p 66. (d) Oelkrug, D.; Flemming, W.; Fullerman, R.; Gunter, R.; Honnen, W.; Krabichler, G.; Schafler, S.; Uhl, S. *Pure Appl. Chem.* **1986**, *58*, 1207 and references therein. (e) Oelkrug, D.; Flemming, W.; Fullerman, R.; Gunter, R.; Uhl, S. In *Fluorescence Spectroscopy, New Methods and Applications*; Wolfbeis, O. S., Ed.; Springer: Berlin, 1993; p 65 and references therein.

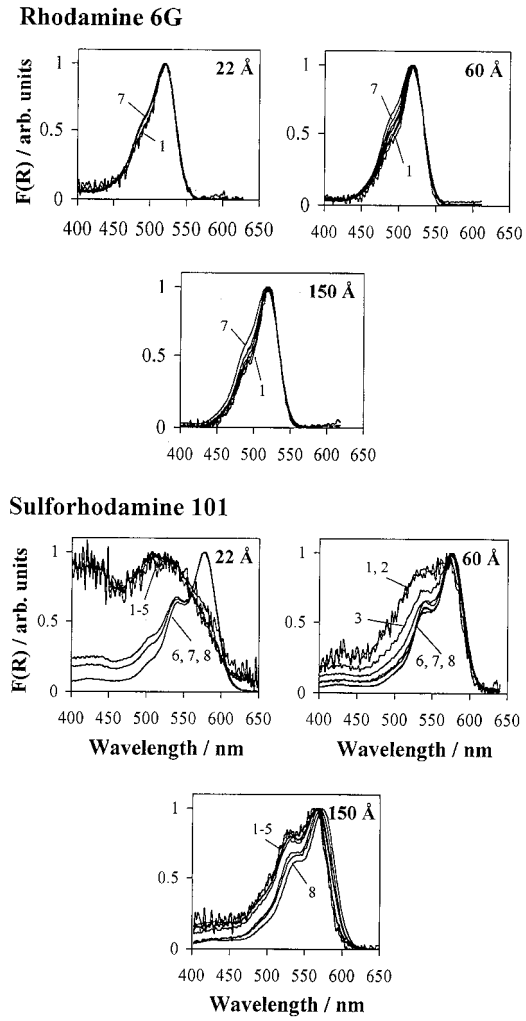

Figure 4. Remission function values for sulforhodamine 101 and rhodamine 6G adsorbed on silicas with 22, 60, or 150 Å pore diameters for the range of concentrations under study, 1 (0.004 μmol g^{-1}) to 8 (0.1 μmol g^{-1}). Spectra are normalized to the maximum of the absorption of the dye. (All samples are type I.)

All spectra are normalized to the maximum absorption. Adsorption onto silica or cellulose clearly changes the relative weight of the vibronic bands and also produces an hypsochromic shift for silica and a bathocromic shift for cellulose relative to the ethanolic solution. This behavior in the cellulosic substrate was previously reported by us[1] and is related with entrapment and hydrogen bond formation of the type cellulose−dye−cellulose. The behavior in silica is a bit more unexpected since the strong interactions with the hydroxyl groups should exist both on cellulose and silica surfaces. Some other effect is certainly present and is responsible for this deviation for shorter wavelengths. Type I and type II samples are similar from the point of view of optical absorption although the deposition of the dye by solvent evaporation (type I) seems to promote a slight increase in the dye aggregation.

An overview of the influence of the silica pore size in the absorption properties and spectra of the two rhodamine dyes is presented in Figure 4, where all spectra are normalized to the absorption maximum. Clearly new absorbing bands are present for low loadings in the sulforhodamine 101 case and especially for small pore silicas. For rhodamine 6G, spectra are similar for all the pore sizes of the silica and only a small increase in the H aggregates presence is detected for the higher loaded samples.

In the case of rhodamine 6G, for all silicas under study, and despite the small scattering coefficients ($S = 10$ cm^{-1} for 150 Å silica, $S = 12.5$ cm^{-1} for 60 Å silica, and $S = 22$ cm^{-1} for 22 Å silica), $F(R)$ is always linear with concentration and the curves are superimposed for the three silicas as can be seen in Figure 2a). This shows that, at the excitation wavelength, there is no significative amount of transmitted light for the cells used in this work (1 cm path length in most cases). This assumption was experimentally verified, and we determined values between 3 and 2.5% for diffuse transmission for the pure silicas. For all samples with adsorbed dye (and specially for low loadings), the diffuse transmitted detected light was always smaller and negligible in most cases. Obviously the diffuse transmitted light was zero for high loadings of the dye.

This clearly shows that the loss of linearity observed in Figure 2b for SR101 and the fact that the curves are not superimposed are not originated by the existence of transmitted light in these samples.

Reflectances were determined with two areas of irradiation (the Cary 14 used in this work has two slits with approximately 1 and 2 cm^2, easily interchangeable). Within an experimental error of ±0.5%, the obtained reflectances were the same for all samples.

3.2. Luminescence Studies of Sulforhodamine 101. We recently reported fluorescence emission studies of rhodamines[1a−c,3a] and other dyes[1a] at room temperature when these dyes are adsorbed onto microcrystalline cellulose and other powdered solid substrates. In the case of sulforhodamine 101 and rhodamine 6G no significative phosphorescence was detected for any of the samples at room temperature when exciting at 337 nm with a nitrogen laser, as compared to fluorescence emission.

According to eq 3 a nice correlation of fluorescence emission intensity (I_F), measured as the total area under

$$I_F = GI_0(1 - R)f_{dye}\phi_F \qquad (3)$$

the emission spectra as a function of the light absorbed by the dye at the excitation wavelength, $(1 - R)f_{dye}$, is expected and was indeed found whenever the luminescent probes exist exclusively in the form of monomers.[1] In eq 3, G is a geometrical factor, I_0 is the excitation intensity at the excitation wavelength, R is the reflectance measured at the excitation wavelength, f_{dye} is the fraction of the excitation light absorbed by the dye at the excitation wavelength, and ϕ_F is the fluorescence quantum yield. Alternatively, I_F versus the square root of the concentration of the dye is also linear for small fractions of absorbed light (see eqs 1−3 for R close to unity at the excitation wavelength or ref 1b). Deviations from linearity may occur for high loadings of dye due, in many cases, to aggregate formation, which are usually nonfluorescent.[1b,c] Dimer emission was also reported in one case.[1a]

The curves for the variation of intensity of fluorescence of sulforhodamine 101 for type I and type II samples as a function of $(1 - R)f_{dye}$ for the dye adsorbed onto 22 Å silica from ethanol are coincident within experimental error. This clearly shows that the two methods for sample preparation provide similar samples from the point of view of its emission properties, provided $(1 - R)f_{dye}$ at the excitation wavelength is the same for type I and type II samples. The fluorescence quantum yield for the same dye entrapped into cellulose is larger ($\phi_F = 1.0$ [9]), reflecting higher rigidity and planarity in this substrate. Figure 5 (top) presents similar results for the same dye adsorbed

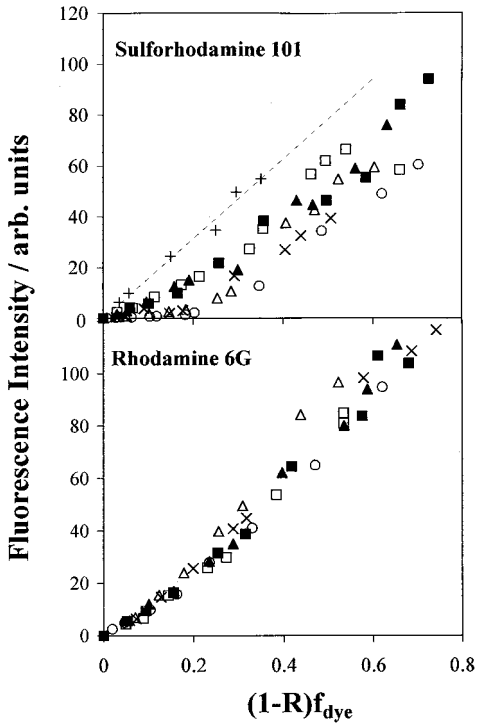

Figure 5. Fluorescence intensity (measured as the total area under the corrected emission spectrum, I_F) as a function of $(1 - R)f_{dye}$ (see text) for sulforhodamine 101 and rhodamine 6G adsorbed onto silica with (□) 150 Å, (▲) 100 Å, (■) 60 Å, (×) 40 Å, (△) 25 Å, and (○) 22 Å pore diameters. (R values are measured at 540 nm for sulforhodamine 101 and 495 nm for rhodamine 6G.) (+) Sulforhodamine 101 on microcrystalline cellulose (dotted line).

onto 22, 25, 40, 60, 100, and 150 Å silicas, while Figure 5 (bottom) refers to rhodamine 6G. A clear dependence of the fluorescence emission quantum yield on pore size becomes, in this way, evident for both dyes.

Equation 3 is written for a simple fluorescent component and can obviously be extended to multiple component systems, as we did in the case of acridine orange where monomers and dimers are emissive (ref 1a and references quoted therein). So, we can write

$$I_F = GI_0(1 - R)\sum_i f_i\phi_{F_i} \qquad (4)$$

In this equation the normal fluorescence quantum yield is replaced by a "weighed" fluorescence quantum yield $\sum_i f_i\phi_{F_i}$, which takes into account the existence of several emitting and nonemitting species.

Using a homemade fluorometer (reflection geometry) described in detail in ref 18, using also as standards for fluorescence quantum yield determination R101, R6G, or SR101 on cellulose (see refs 1a−c), and also by the use of eqs 3−5, we determined $\sum_i f_i\phi_{F_i}$ or ϕ_F for the above-mentioned samples. In this sense the experimentally determined fluorescence yields reflect the formation of nonplanar and nonemissive species and include the information of the fraction f_i of the fluorescent compound. The "weighed" fluorescence quantum yields quoted before were simply obtained from slopes of I_F versus $(1 - R)f_{dye}$, when compared with the equivalent slope obtained for cellulose (where $\phi_F = 1.0$ was assumed both for SR101 and R6G).

As reported before,[1] fluorescence quantum yields of probes adsorbed onto powdered solids can be determined by the use of eq 5, where the superscripts u and s refer to the unknown and standard samples.

$$\sum_i f_i^u\phi_{F_i}^u = \phi_F^s\frac{I_F^u(\lambda_e)(1 - R_s^{\lambda_e})f^s I_0^s(\lambda_e)}{I_F^u(\lambda_e)(1 - R_u^{\lambda_e})I_0^u(\lambda_e)} \qquad (5)$$

$I_0^s(\lambda_e)/I_0^u(\lambda_e)$ can be easily obtained provided the energy profile of the system is accurately determined.[18] Rhodamine 101 or sulforhodamine 101 onto microcrystalline cellulose can be used as reference compounds ($\phi_F^s = 1.0$). The reasons for that were previously reported in refs 1b,c and 9.

As a general comment, sulforhodamine 101 "feels" much more the silica surface influence than rhodamine 6G, in the sense that it exhibits a larger decrease in ϕ_F and especially for low loadings of the dye. Comparing with the sulforhodamine 101/microcrystalline cellulose curve presented in Figure 5 (top), we can see that, for high loadings of rhodamine 6G in Figure 5 (bottom), ϕ_F approaches unity, while, for low loadings of this dye, only a slight decrease of ϕ_F can be noted, very slightly dependent on the silicas pore size. It probably reflects different degrees of rigidity of the entrapped dye molecules into the different size pores.

Please note that the behavior predicted by eq 3 (linear variation of I_F versus $(1 - R)f_{dye}$) is verified in practice for rhodamine 6G and for all silicas, independently of the S values for each silica, as Figure 5 (bottom) shows.

The most important negative deviations from linearity occur in the SR101 case and are more important in the 22 Å silica, where the scattering coefficient is the highest (22 cm^{-1} in the 22 Å against 10 cm^{-1} in the 150 Å silica), as Figure 5 (top) shows.

As we said before, fluorescence experiments were carried out in 1 cm silica cells (section 1 × 1 cm, 4 cm high). However, 2 × 1 and 0.5 × 1 cm cells were also used for fluorescence experiments. For high loadings, the three types of cells gave the same results. Even for low loadings, no significative differences were detected within experimental error, showing that, at the excitation wavelength (λ = 540 nm for SR101 and λ = 495 nm for R6G), the lateral diffusion of light is not important and eqs 3 and 4 are valid for the present study. For most samples, the amount of absorbed light by the rhodamines is predominant, eliminating the disadvantage of the substrate's small scattering coefficients used in this work.

Deviations from linearity and specially interesting and important effects occur in the 22 Å silica, the one with the highest S. The 150 Å silica samples exhibit an almost linear behavior of I_F versus $(1 - R)f_{dye}$, despite the smaller S.

The fluorescence measurements were performed in our homemade spectrofluorometer (described in ref 18) which allows us to use different areas of illumination. In the present case spots from about 5 mm^2 experiments to about 0.8 cm^2 were used. The standard area of irradiation was 0.4 cm^2. The results were similar to the ones presented in Figure 5, within experimental error.

It is important to emphasize several relevant features: First, the initial slope (from the initial linear region) for sulforhodamine 101 on 22 Å silica is the smallest one ($\sum_i f_i\phi_{F_i} = 0.08 \pm 0.03$), as is clearly shown in Figure 5 (top). The "weighed" fluorescence quantum yields ($\sum_i f_i\phi_{F_i}$) determined were 0.10 ± 0.03, 0.20 ± 0.05, 0.35 ± 0.05, 0.42 ± 0.05, and 0.50 ± 0.10 for low loadings and for 25, 40, 60, 100, and 150 Å silicas, respectively. For high loadings $\sum_i f_i\phi_{F_i} = 0.70 \pm 0.10$. These values for ϕ_F can be compared with the value of about 0.70 obtained for rhodamine 6G in all silicas (low loadings) and an unitary ϕ_F for high loadings. These "weighed" fluorescence quantum yields are always calculated by determining slopes for low or high loadings,

using eqs 3−5, and taking sulforhodamine 101 or rhodamine 101 or 6G on cellulose as references as studied before.[1b,c]

Rhodamine 101 behaves in the same way as sulforhodamine 101 in what concerns the luminescence pore size dependence.

Sulforhodamine 101 on microcrystalline cellulose from ethanol, where the dye is entrapped within the polymer chains,[1b,c] and in this way only physically adsorbed, is the sample which presents the largest fluorescence quantum yield ($\phi_F = 1.00 \pm 0.03$). This fact is consistent with a previously described picture, the use of ethanol, a polar and protic solvent, as a swelling agent for microcrystalline cellulose allowed us to entrap sulforhodamine 101 within the polymer chains. This provides a rigid environment capable of causing only a small enhancement of the fluorescence of this dye when compared with the solution case at room temperature ($\phi_F = 0.96 \pm 0.03$).[4] With other dyes, the enhancement of ϕ_F can reach several orders of magnitude.[1,3]

All the results presented in paragraphs 3.1 and 3.2 point to the formation of sulforhodamine 101 conformers. The spectroscopic evidence presented until here, ground-state absorption data as well as "weighed" fluorescence quantum yields from physically adsorbed samples, provide evidence for the occurrence of a strong and differentiated interaction of the probes with the silica substrates. The smaller the pore size of the activated silica, the larger is the formation of ground-state nonplanar conformers, which absorb at shorter wavelengths due to the decrease in conjugation. These conformers do not emit luminescence. The probe−silica interaction is stronger for the rigidified rhodamine; therefore, more conformer is formed in this case.

Other experiments were performed with neutral and acidic alumina (with 58 Å diameter pores in both cases) to test the possibility of protonation, H-bonding, or chemiadsorption, as these surfaces are well-known for strong interaction with adsorbed probes (see for instance the excellent papers of Oelkrug's group on this matter, refs 22d,e and references therein). No species other than the monomers were detected in both substrates, thus pointing to nonplanar conformer formation on silica as described before.

3.3. XPS Studies. The XPS studies of sulforhodamine 101 and rhodamine 6G adsorbed on silica gel were mainly centered on the nitrogen region (N 1s) for the dye and on the silicon region (Si 2p) for the substrate. In fact, every sample prepared in "ex-situ" conditions presents small amounts of organic contamination containing carbon and oxygen. Nitrogen and sulfur are then the most representative elements of the dye molecules. On the other hand, since nitrogen electrons can be involved in the delocalized π system, nitrogen is a good element to provide information about conformational changes or intermolecular interactions which may contribute to modify the nitrogen density charge. As an example, a large planarity corresponds to a large participation of nitrogen atoms in the delocalized π system; a high positive charge is, in this case, located at each one of the nitrogen atoms that are bound to the xanthenic group and the binding energy increases. Inversely, if alkyl groups are out of the xanthenic plane, the electronic density around those nitrogen atoms will increase and the N 1s binding energy decreases; also, the presence of hydrogen bonds involving the nitrogen atom increases the N 1s binding energy.[3,20]

Sulfur atoms are also present exclusively in the sulforhodamine dye molecule, but they are not so useful as nitrogen atoms, because they are far from the xanthenic part of the molecule and do not participate in the conjugated system.

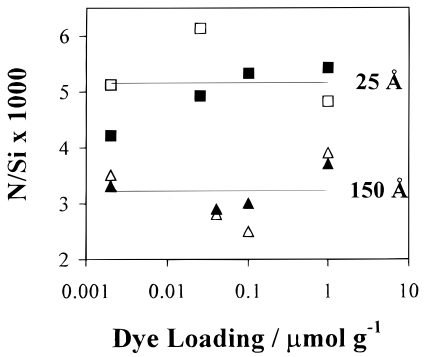

Figure 6. Atomic ratio N/Si for sulforhodamine 101 (closed symbols) and rhodamine 6G (open symbols) adsorbed on 25 or 150 Å pore silicas as a function of dye concentration. Straight lines in the plot represent average values.

(a) Quantitative Analysis. The dyes used in this work, were sulforhodamine 101 and rhodamine 6G. The dye loadings under study were 0.002, 0.025, 0.10, and 1.0 mol g^{-1} onto silica gel with 25 Å pores and 0.002, 0.04, 0.10, and 1.0 mol g^{-1} onto silica gel having pores of 150 Å diameter. Within the error associated with XPS quantifications, we showed that the atomic ratio N/Si is constant and independent of dye loading as we show in Figure 6 (although a slight variation is detected for sulforhodamine adsorbed on 25 Å pore silica). That ratio is also larger in the silica having 25 Å pores than in the silica having 150 Å pores (by a factor around 1.5).

The specific areas for the two referred silicas are respectively 600 and 300 m^2/g. Therefore, if the probe distribution over the whole silica particle was homogeneous, it would be expected that, first, the N/Si ratio should increase with the dye loading (the atomic N/Si stoichiometric ratio is about $1.2 \times 10^{-4}c$, c being the dye loading in μmol/g of silica) and, second, it should be lower in the silica having larger specific area for the same dye loading. The experimental observation is exactly the inverse.

The value of the atomic ratio measured from XPS data being of the order of 10^{-3}, much larger than the stoichiometric ratio, especially for the low loaded samples, shows that, for these samples, the dye must be mainly adsorbed near the extreme surface of the pores. It also shows that the fraction of external surface occupied by dye molecules remains constant for higher loadings. This is compatible with an adsorption occurring essentially in depth (filling the pores) and not with an increase in the number of the occupied pores with increasing loadings. Moreover, the mean depth of adsorption is larger for the larger pore diameter silicas which is indicative of a larger penetration of dye molecules into the pores, the constraints concerning penetration being more important in the 25 Å pore silica than in the 150 Å pore silica.

The order of magnitude of the number of pores emerging at the extreme surface was estimated by computing lower and upper limits corresponding respectively to a system of nonintersecting cylindrical capillaries within cubic particles and to cubic particles having the whole external area occupied by pores. This approach showed that for all the dye loadings used in this study the number of dye molecules is larger than the number of emerging pores except, perhaps, for the lowest loading in the case of the silica having 22 Å pore diameter. This means that XPS results are compatible with the occupation of all the pores, even for low loadings of dye.

(20) Kerber, S. J.; Bruckner, J. J.; Wozniak, K.; Seal, S.; Hardcastle, S.; Barr, T. L. *J. Vac. Sci. Technol., A* **1996**, *14*, 1314.

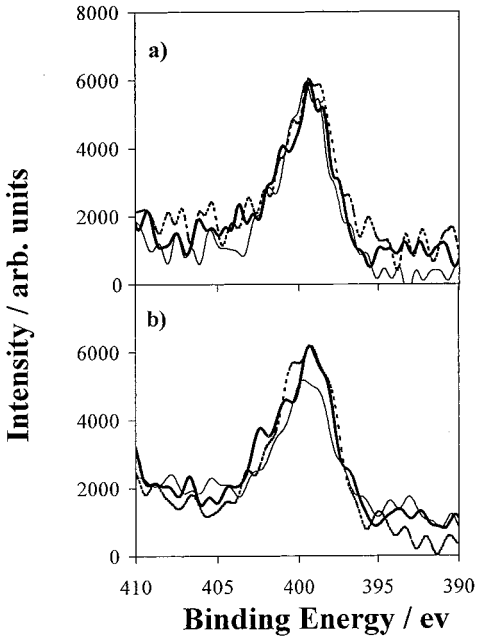

Figure 7. XPS spectra for the N 1s region of samples of the two rhodamines adsorbed on 25 Å silica. (a) Sulforhodamine 101: (—) 0.002 μmol g^{-1}; (—) 0.025 μmol g^{-1}; (- - -) 0.1 μmol g^{-1}. (b) Rhodamine 6G: (—) 0.002 μmol g^{-1}; (—) 0.020 μmol g^{-1}; and (- - -) 0.1 μmol g^{-1}. (All samples are type I.)

(b) Qualitative Analysis. In what concerns the analysis of the N 1s peak, its shape remains practically unchanged with dye loading, as we can see in Figure 7. This means that, first, the decrease in delocalization evidenced by UV−vis experiments for low loadings of sulforhodamine adsorbed on 25 Å pore diameter does not imply a measurable change in electronic density charge around the nitrogen atom. This finding does not rule out the participation of nitrogen atom in the phenomena of breaking the delocalization. When nitrogen stops participating in the system and loses its positive charge character, its XPS N 1s binding energy should decrease. Simultaneously, its valence orbitals change from sp^2 to sp^3. This change in hybridization usually implies an increase in XPS binding energy (e.g., in the aromatic C 1s, BE = 284.4−284.7 eV and, in the aliphatic C 1s, BE = 285 eV).[21] Apparently, the two effects may compensate. Second, the interaction between dye molecules and the substrate leading to the dye molecule deformation, thence decreasing the delocalization, does not involve the nitrogen atom as much as it did in the case of the rhodamine dyes covalently bound to cellulose.[3a]

Obviously, given the weakness of the N 1s signal and, therefore, the large time of X-ray irradiation (~100 min) needed to have measurable signals, we cannot rule out the possibility of breaking a hydrogen bond between the dye and the substrate. However, for a film of sulforhodamine, spread from an alcoholic solution on a silicon wafer, no changes on the N 1s peak were detected for the first 15 min. Even the vacuum could also have an effect over the measured concentration of the dye allowing for the least bonded molecules (not entrapped into the pores or placed near the top entrance of the pores) to evaporate. Anyway, a sample analyzed by diffuse reflectance absorption from the fundamental state, before and after being submitted to a high vacuum (~10^{-8} mbar) during 24 h, gave unchanged spectra within experimental error.

Due to the fact that XPS only "sees" surface layers of about 100 Å width, one may be tempted to think that we mainly see probe molecules poorly interacting with the silica surface and that the strongest interactions occur deeply inside the pore. However, type I washed samples, where all the strictly physically adsorbed monomers were removed by the ethanolic washing procedure, leaving only molecules strongly interacting with the surface (conformers), provide similar XPS spectra.

3.4. Final Remarks. UV−vis experiments provide a clear evidence for a decrease in conjugation in rigid rhodamines adsorbed onto small pore silicas, thus pointing to nonplanar conformer formation following very strong interactions with the silica porous surface. This effect is not so relevant for silicas with larger pores. Rhodamine 6G, where the alkyl groups are not rigidly bound to the xanthenic part of the molecule, does not evidence this effect probably due to stereochemical restrictions imposed by the aliphatic substituting groups. However, even in this case, a tiny decrease in the luminescence of the probe at low loadings was detected, depending on pore size. It probably reflects smaller rigidity of the probe inside larger pores (therefore less luminescence) when compared with smaller pores.

Quantitative and qualitative XPS analysis also provide important information about this pore size effect. The best insight we may have into the adsorption mechanism of sulforhodamine on porous silica from XPS experiments is the evidence for multiple occupation of the pores, as well as a deeper penetration into the pores especially in the case of the silicas with larger pores. Thus, the probe surface concentration measured by XPS becomes larger in the case of the silica with the larger surface area.

4. Conclusions

X-ray photoelectron spectroscopy and UV−vis absorption and luminescence studies proved to be complementary techniques in the study of rhodamine dyes adsorbed onto silica. This allowed us to establish a clear picture of the specific interactions of sulforhodamine 101 and rhodamine 6G with this substrate.

UV−vis ground-state diffuse reflectance absorption and luminescence studies of sulforhodamine 101 showed a significant decrease of fluorescence emission quantum yield when this probe is adsorbed on porous silica, due to stereochemical constraints and formation of nonplanar, nonemissive conformers.

X-ray photoelectron studies provided evidence for different depths of deposition of dye molecules here assigned to different constraints concerning dye molecule penetration into the pores.

All the results presented led us to conclude that the size of the pore plays a predominant role on the formation of nonplanar conformers, deeply affecting the luminescent properties of the dyes.

Acknowledgment. We acknowledge M. I. Morais for her technical support on sample preparation for XPS analysis and A. R. Garcia for some preliminary experiments with rhodamine 101 on silica. M.J.L. thanks the JNICT for her Ph.D. grant. Equipment was financed by Project Praxis/2/2.1/QUI/22/94.

LA9908182

(21) Beamson, G.; Briggs, D. *High-resolution XPS of Organic Polymers. The Scienta ESCA300 Database*; John Wiley and Sons: Chichester, U.K., 1992; p 158.